THE JOURNAL OF PHYSICAL CHEMISTRY C

Article

pubs.acs.org/JPCC

Dimethyl Disulfide on Cu(111): From Nondissociative to Dissociative Adsorption

Xiao-Li Fan,*[,†,‡] Yan Liu,[†] Run-Xin Ran,[†] and Woon-Ming Lau*[,‡,§]

[†]School of Materials Science and Engineering, State Key Laboratory of Solidification Processing, Northwestern Polytechnical University, 127 YouYi Western Road, Xi'an, Shaanxi 710072, China

[‡]Beijing Computational Science Research Center, Beijing 100084, China

[§]Chengdu Green Energy and Green Manufacturing Technology R&D Center, Chengdu, Sichuan 610207, China

ABSTRACT: Adsorption of dimethyl disulfide (CH_3SSCH_3) on Cu(111) was investigated using the density functional theory method. This computational work clarifies some hitherto unclear issues about nondissociative adsorption of CH_3SSCH_3. In addition, the work charts the reaction pathways and relevant transition states about CH_3SSCH_3 dissociation. Briefly, our results show that trans-CH_3SSCH_3 is 0.5 eV more stable than its cis-isomer in gas phase, and the domination of the trans-isomer in population is maintained for CH_3SSCH_3/Cu(111) as its adsorption energy of 0.42 eV is 0.23 eV higher than that of the cis-isomer. Our calculations also clarify that trans-CH_3SSCH_3 nondissociatively chemisorbed on the top sites of Cu(111), with the S−S bond aligning along the nearest Cu−Cu bond. The details of these and other adsorption properties are further elaborated with our computational electronic structures and simulated scanning tunneling microscopic images. In addition, our reaction dynamics analysis shows that the dissociation of trans-CH_3SSCH_3 to form CH_3S/Cu is barred by an activation barrier of 0.21 eV, but since it is exothermic by 1.1 eV, the dissociation can proceed although the surface temperature cannot be too far below room temperature. This explains the experimental findings that intact trans-CH_3SSCH_3 is the only product for CH_3SSCH_3/Cu(111) at 5 K and implies that the experimentally observed CH_3SSCH_3 dissociation at 150 K was probably influenced by other factors such as the presence of intrinsic surface defects.

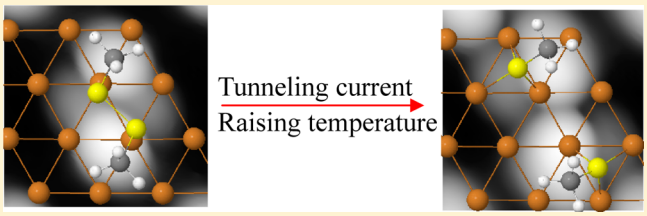

1. INTRODUCTION

Self-assembly monolayers (SAMs) offer a convenient route to modify surfaces with tailored properties that have applications in surface patterning, corrosion prevention, nanotechnology, biosciences, and molecular electronics.[1−7] Most attention has been devoted to the SAMs of alkyl thiolates on noble metal surfaces with high surface symmetry and stability. In general, alkyl thiolate SAMs can be grown either from disulfides (RSSR) or alkyl thiols (RSH), and experiments have indeed demonstrated that the two reactants yield equivalent SAMs.[8,9] It was believed that the RS−SR bond in the case of RSSR adsorption and the S−H bond in the case of RSH adsorption are broken spontaneously upon adsorption. However, recent experimental data and theoretical calculations do not support this spontaneous dissociation model.[10−15] For example, recent density functional theory calculations found stable nondissociatively adsorbed configurations for short-chain alkylthiols[16−18] and benzenethiol[19] on Au(111). Interestingly, the stability of nondissociative adsorption is also coverage dependent. For example, the adsorption energies for nondissociatively adsorbed alkylthiols are ∼0.44−0.48 eV at low coverage and they change to ∼0.18 eV at high coverage.[16] In short, further studies and understanding of adsorption details are required before one can control the chemistry and structures of thiol and dithiol SAMs.

In this work, we examine these issues by taking adsorption of dimethyl disulfide (CH_3SSCH_3) as a model system. We use dimethyl disulfide not only because it is simple and easy to prepare, and can be formed even in air or in solution, but also because dithiol SAM formation is known[20] to be more sensitive to the self-assembly conditions than the case of thiol SAM formation. In addition, such a model system has also been adopted in several previous studies. For example, the adsorption of CH_3SSCH_3 has been studied by scanning probe imaging[21] and high-resolution electron energy loss spectroscopy (HREELS)[22] as well as by computation.[22−24] Most of these experimental and computational results explain various facets of the S−S bond dissociation and the subsequent adsorption of CH_3S on Au(111). Although nondissociative adsorption of CH_3SSCH_3/Au(111) was computationally examined by Hayashi et al.,[22] Grönbeck et al.,[23] and Wang et al.,[24] these previous studies again focus more on the descriptions of the dissociation of the nondissociative adsorption precursor than on describing the nondissociative adsorption. In fact, their categorical assignment of nondissociative adsorption to physisorption is not supported by any analysis of the chemical nature of the adsorbate−adsorbant

Received: November 21, 2012
Revised: March 8, 2013
Published: March 11, 2013

dx.doi.org/10.1021/jp311481d | J. Phys. Chem. C 2013, 117, 6587−6593

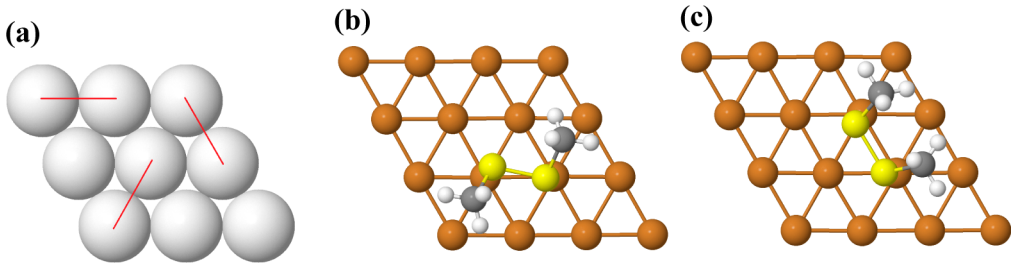

Figure 1. (a) Three adsorption sites for CH_3SSCH_3 on Cu(111) (red lines represent the S−S bond). (b) Top view of trans-CH_3SSCH_3 adsorbed on Cu(111). (c) Top view of cis-CH_3SSCH_3 adsorbed on Cu(111).

interactions. In this regard, the recent high quality experimental data with scanning tunneling microscopy (STM) to track the molecular interactions in nondissociative adsorption of CH_3SSCH_3/Cu(111) and the relevant dissociation properties are critically important in advancing the knowledge of CH_3SSCH_3/Cu(111) adsorption.[10−12] For example, the detailed surface structures of nondissociative adsorption of trans-CH_3SSCH_3 were observed on Cu(111) by STM at 5 K[10] with an atomic resolution good enough to identify the exact adsorption locations of the two CH_3 groups. In fact, nondissociative adsorption of trans-CH_3SSCH_3/Au(111) was also studied with STM by at 5 K[11] and 10 K[12] such that CH_3SSCH_3/Cu(111) and CH_3SSCH_3/Au(111) can be compared. Moreover, the field of dithiolate and thiolate adsorption continues to develop, with new experimental data and theoretical models.[25−32] An emerging trend in this development is the venture into discussion about reaction pathways and dynamics, effects of coverage, intrinsic defects on the substrate, and adsorption-induced reconstruction.

The present work aims at addressing some unsettled issues on thiol SAMs, with CH_3SSCH_3/Cu(111) as a model system and with the first-principles method as the analysis tool. Although copper is a practical substrate for SAM formation, there has been much less attention paid to thiolates on copper[28,33] in comparison to the ubiquitously studied thiolate−gold interface. In this work, we examined the nondissociative adsorption of trans-CH_3SSCH_3 and its cis-isomer on Cu(111), as well as the electronic structures and the simulated STM images, to clarify the interpretation of the reported experimental observations. The coverage cases of 1/16 and 1/20 monolayer were examined and compared, and the effect of adsorption-induced reconstruction was checked for these two low coverage cases. We also investigated the dissociation pathways to study the mechanisms of S−S bond dissociation. By comprehensively studying the sites and energetics of the nondissociative adsorption and the dissociative reaction pathways leading to CH_3S/Cu adsorption, we attempt to bridge the knowledge gap that exists so far in the study of the dialkyl disulfide adsorption.

2. COMPUTATIONAL METHODS

The first-principles calculations were performed by using the Vienna ab initio simulation package (VASP)[34−37] based on the density functional theory (DFT).[38,39] In these calculations, the electron−ion interactions were described by the projector augmented wave (PAW) method.[40,41] The generalized gradient approximation (GGA)[42] of the Perdew−Burke−Ernzerhof (PBE) formula was used for the electronic exchange-correlation potential. The wave functions were expanded in a plane wave basis with an energy cutoff of 400 eV. With the calculated density of states (DOS) data of a specific adsorption geometry, STM images were simulated using the Tersoff−Hamann's formula and its extension.[43] Finally, for the calculations of reaction pathways and transition energy barriers, the minimum energy paths (MEPs) were mapped out using the nudged elastic band (NEB) method developed by Jónsson and coworkers.[44,45]

Our calculated lattice constant for the Cu bulk is 3.61 Å, in agreement with the experimental value of 3.61 Å.[46] The Cu(111) surface was modeled as a (4 × 4) supercell with 10.22 × 10.22 Å in the *xy*-plane and 21.26 Å in the *z*-direction to simulate the low coverage of 1/16. For the analysis of coverage dependence, a (4 × 5) supercell was used to model the coverage of 1/20. The Monkhorst−Pack of a 3 × 3 × 1 mesh was used to sample the first Brillouin zone. In the total energy calculations, the Cu atoms of the bottom layer were fixed at the bulk positions, while the adsorbed molecule and the other three layers of Cu atoms were fully relaxed. The convergence criteria of 0.03 eV/Å in the total energy and the minimum energy paths (MEP) calculations were adopted.

3. RESULTS AND DISCUSSION

3.1. Details of Nondissociative Adsorption of CH_3SSCH_3 on Cu(111). To set a platform for studying the adsorption of CH_3SSCH_3, we first clarify the properties of free CH_3SSCH_3 in gas phase. Our computational results agree very well with the previous ab initio molecular orbital studies,[47] experimental microwave spectroscopy,[48] and experimental electron diffraction[49] studies in that free CH_3SSCH_3 has two stable isomers: trans- and cis-CH_3SSCH_3, with the trans-isomer 0.50 eV more stable than the cis-isomer. This means that under normal conditions trans-CH_3SSCH_3 is dominating in population. A rise in temperature leads to an increase of the relative population of cis-CH_3SSCH_3 due to thermal excitation. As for molecular geometry, the respective C−S−S−C dihedral angles are 87.0° and 0.4°, the S−S bond distances are 2.03 and 2.13 Å, and the S−C bond distances are 1.82 and 1.80 Å for the trans- and cis-isomer.

For adsorption on Cu(111), there are three groups of high-symmetry adsorption sites: top site, fcc and hcp hollow site, and bridge site. The distances between the nearest top sites and nearest bridge sites are both 2.56 Å. But the distance between the nearest hollow sites is 1.48 Å. A comparison of these data with the S−S distance in trans-CH_3SSCH_3 in gas phase (2.03 Å) offers some clue on CH_3SSCH_3 adsorption on Cu(111). If each S atom of CH_3SSCH_3 molecule binds to the top Cu atom, the S−S distance will be elongated. A similar change will happen when the two S atoms adsorb on the bridge sites. However, the molecule structure of CH_3SSCH_3 will be compressed upon the adsorption on the hollow sites. In this

dx.doi.org/10.1021/jp311481d | J. Phys. Chem. C 2013, 117, 6587−6593

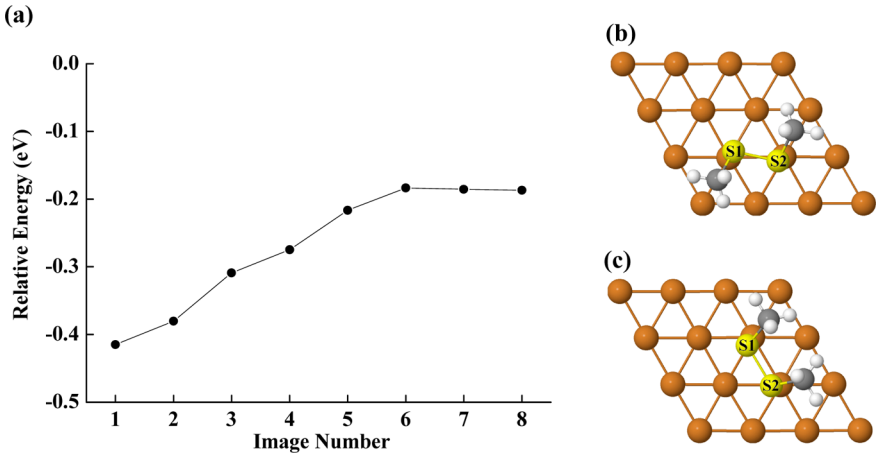

Figure 2. (a) Minimum-energy path along reaction Path_I for the rotational motion of one CH_3S group of adsorbed CH_3SSCH_3 on Cu(111). (b) Top view of the initial trans-isomer. (c) Top view of the final cis-isomer.

work, we investigated the above three scenarios of adsorption: adsorption on the adjacent top sites, bridge sites, and hollow sites. It turns out that the top site adsorption of CH_3SSCH_3 is the most stable. As shown in Figure 1a, there are three adsorption locations for the top site adsorption in one unit cell. On each of these three adsorption locations, the S−S bond of the top site adsorption orientates along the Cu−Cu bond with each pair of S atoms staying on a pair of adjacent top sites.

For the adsorption of CH_3SSCH_3 on Cu(111), after the structure optimization, the adsorption energies were calculated as

$$E^{f}_{CH_3SSCH_3} = E(\mathrm{Cu}) + E(CH_3SSCH_3) - E(CH_3SSCH_3/\mathrm{Cu})$$

where E(Cu), $E(CH_3SSCH_3)$, and $E(CH_3SSCH_3/\mathrm{Cu})$ are the respective energy terms of the copper surface, CH_3SSCH_3 molecule, and adsorbed surface with CH_3SSCH_3.

We have calculated the top site adsorption configurations of trans-CH_3SSCH_3/Cu(111) on all the three locations shown in Figure 1a. It turns out that those configurations are energy equivalent; Figure 1b shows one of them. For the three equivalent top-site configurations, the S−S bond distances elongated by about 0.06 Å upon adsorption, and the distances between S and the adsorbed Cu atoms are 2.39 Å. The dihedral angle of C−S−S−C increases to 112.3° from the original value of 87.0°. The adsorption energies are all about 0.42 eV. Upon the adsorption of CH_3SSCH_3, the two adsorbent Cu atoms are lifted by about 0.15 Å, and the Cu−Cu bond distance increases to 2.63 Å from the original value of 2.56 Å. The nearest distances between the adjacent Cu atoms and the adsorbent Cu atoms also increase by 0.03−0.14 Å.

Although cis-CH_3SSCH_3 is 0.5 eV less stable than trans-CH_3SSCH_3 in gas phase, this energy difference alone does not rule out the possibility that cis-CH_3SSCH_3 can participate actively in the overall picture of CH_3SSCH_3/Cu(111). For example, it is known that while singlet oxygen is less stable than triplet oxygen by 0.98 eV in gas phase, it still plays a very important role in adsorption-induced surface reactions on silicon.[50] The adsorption geometry cis-CH_3SSCH_3 on Cu(111) is shown in Figure 1c. The adsorption energy of this configuration is 0.19 eV. The S−S bond distance is about 2.17 Å, and the distances between S and the adsorbed Cu atoms are 2.38 Å. To elaborate on the likelihood of isomerization of trans-CH_3SSCH_3/Cu(111) to its cis-isomer, we depict in Figure 2 our computational results on the relevant rotational motion of the C−S axis of CH_3S along the S−S axis. More specifically, Path_I describes the rotational motion of one CH_3S group of CH_3SSCH_3/Cu(111) in the process of isomerization between the trans- and cis-isomer, with the MEP and motion trace shown in Figure 2. The analysis reveals that the transformation of trans-CH_3SSCH_3/Cu(111) to its cis-isomer is endothermic by 0.23 eV with a virtually no energy barrier, as shown in Figure 2a. As such, although adsorption of CH_3SSCH_3 on Cu(111) does reduce the energy difference between the trans- and cis-isomer from 0.5 to 0.23 eV, the reduction is not enough to influence the domination of the trans-isomer in low and moderate temperature. More specifically, the cis-isomer population reaches ∼1% when the adsorption temperature rises to 250 °C.

For each of the adsorption configuration shown in Figure 1, an enantiomer can be formed by making a mirror-image copy with the mirror plane normal to the surface and along the S−S axis. We repeated our calculations for these enantiomers and, not surprisingly, could not differentiate them in adsorption energy.

Because STM, particularly STM imaging, is becoming the most effective and popular technique for studying and describing surface adsorption, it is relevant to translate the aforementioned computational results on surface adsorption configurations and relevant electronic structures to simulated STM images. Figure 3 shows the simulated STM images of the most stable top-site configurations of trans- and cis-CH_3SSCH_3/Cu(111), all for electron tunneling from the STM tip to the lowest unoccupied molecular states. In

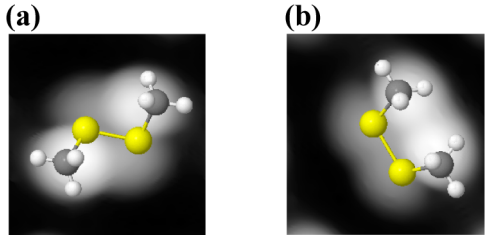

Figure 3. The simulated filled-state STM images at bias voltage of −2.0 V for the adsorption of CH_3SSCH_3 molecule on Cu(111): (a) trans-CH_3SSCH_3; (b) cis-CH_3SSCH_3.

dx.doi.org/10.1021/jp311481d | J. Phys. Chem. C 2013, 117, 6587−6593

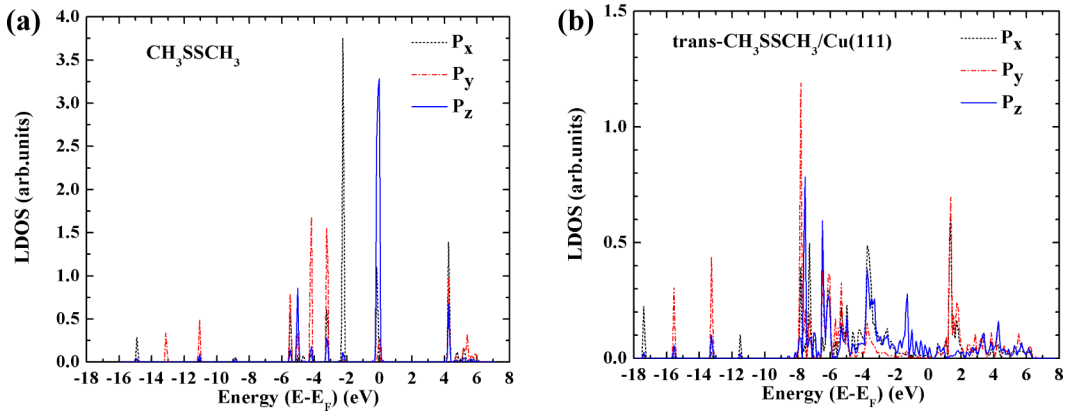

Figure 4. Decomposed local density of states of the S atom in (a) free CH_3SSCH_3 molecule and (b) nondissociative adsorption of CH_3SSCH_3 on Cu(111).

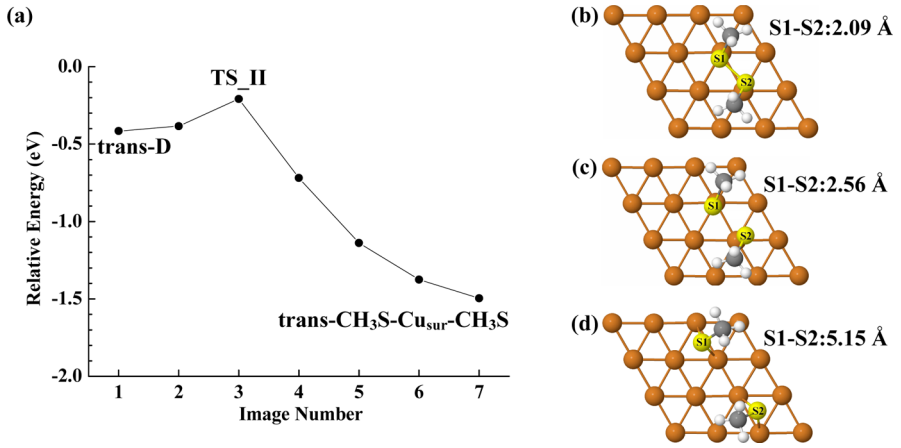

Figure 5. (a) Minimum energy path along reaction Path_II for the dissociation of the trans-CH_3SSCH_3 molecule on Cu(111). (b) Top view of the reactant state along Path_II. (c) Top view of the transition state along reaction Path_II. (d) Top view of the product state with two CH_3S adsorbed on Cu(111) in the trans-conformer along Path_II.

reference to our computational results on local DOS, we interpret that the bright elliptic protrusion lobes in the STM image of each adsorption configuration reflect mainly the location and lowest unoccupied local DOS of the CH_3 groups. With the identification of the location of the CH_3 groups, the pictorial comparison of STM images of the nondissociative top-site adsorption configurations of trans-CH_3SSCH_3/Cu(111) and cis-CH_3SSCH_3/Cu(111), as shown in Figure 3, clearly shows that STM imaging can indeed unambiguously differentiate trans-CH_3SSCH_3/Cu(111) from cis-CH_3SSCH_3/Cu(111). In reference to the known experimental STM study of CH_3SSCH_3/Cu(111) at 5 K in which only trans-CH_3SSCH_3 adsorbed at the top-sites of Cu(111) was observed,[10] our computation results are accurate in that our simulated STM images for the adsorbed trans-CH_3SSCH_3 match the experimental images well and our energy data predict the domination of trans-CH_3SSCH_3/Cu(111) at 5 K. This implies that our computational results on other properties and data about the adsorption of CH_3SSCH_3/Cu(111) are also likely to bear useful insight into issues such as the adsorption configurations and energetics of nondissociative adsorption at other surface sites, the isomerization between trans- and cis-isomer, and dissociation of adsorbed CH_3SSCH_3.

As mentioned in the Introduction, Reimers[24] claimed that the nondissociative adsorption of CH_3SSCH_3 is physisorption in nature. In the present study, the adsorption energy of about 0.4 eV and the relatively short distances between S and Cu indicate that the nondissociative adsorption is actually chemisorption in nature. To settle this issue whether the nondissociative adsorption should be categorized as phyisorption or chemisorption, we further examined our calculation results in electronic structures including local DOSs. The decomposed S 3P DOSs are shown in Figures 4a and 4b for the trans-CH_3SSCH_3 molecule before and after adsorption, respectively. One can see the localized 3P atomic orbitals becoming delocalized after adsorption on Cu(111), with P_z being the orbital that interacts significantly with the substrate Cu atom. More specifically, the interaction changes the position of the highest occupied P_z orbital from −0.2 eV to −1.3 eV and decreases its peak height to 10%. These changes imply the formation of a chemical bond between S and Cu.

3.2. Reaction Mechanism Controlling the Dissociation of CH_3SSCH_3 on Cu(111). In this section, we turn our focus onto the kinetics of the dissociation of CH_3SSCH_3 on Cu(111) by examining the reaction pathway leading to the dissociation of CH_3SSCH_3/Cu into CH_3S/Cu. Briefly, Path_II describes the dissociation reaction of trans-CH_3SSCH_3/Cu(111) into two adsorbed CH_3S groups retaining the original molecular conformation of the trans-isomer.

The calculated MEP and transition state along Path_II are shown in Figure 5. Along the MEP of Path_II, the dissociative reaction starts with the gradual separation of the two methyl

dx.doi.org/10.1021/jp311481d | J. Phys. Chem. C 2013, 117, 6587−6593

groups. In the transition state TS_II shown in Figure 5c, the S−S distance increases to 2.56 Å from the original value of 2.09 Å in the initial nondissociative adsorption, indicating the breakage of the S−S bond. The two CH_3S species resulted from the dissociation of the S−S bond sit on top of a pair of adjacent Cu atoms with a S−Cu bond length of 2.26 Å. The corresponding activation barrier is 0.21 eV. In the final product state, both the two CH_3S species basically adsorb on the bridge sites with slight shift toward the hollow site. The average S−Cu distance is 2.28 Å. The energies and the structure parameters of the initial nondissociative adsorption as well as the transition and dissociated states are summarized in Table 1.

Table 1. Computational Results along Reaction Path_II for the Dissociation of trans-CH_3SSCH_3 on Cu(111)

reference	d_{S-Au}[a] (Å)	d_{S-S} (Å)	E^f_{S-S} (eV)
trans-D	2.39	2.09	0.42
TS_II	2.26	2.56	0.21
trans-$CH_3S-Cu_{sur}-CH_3S$	2.28	5.15	1.50

[a]Average distance between the S atom and the nearest-neighboring surface Cu atom.

It is notable that along the dissociation reaction pathway the two CH_3S groups move away along the parent direction of the S−S bond, with the S−C bond directions in the two CH_3S species maintaining those in the parent CH_3SSCH_3 molecule. Our calculated results agree well with the experimental observations on the dissociation of CH_3SSCH_3 by tunneling current on Au(111) at low temperature in that the dissociation products of the two CH_3S/Au units maintain their original conformations in the parent CH_3SSCH_3/Au.[11]

Since the activation energy of the dissociative path of trans-CH_3SSCH_3/Cu(111) is 0.21 eV and that for isomerization of trans-CH_3SSCH_3/Cu(111) to cis-CH_3SSCH_3/Cu(111) is 0.23 eV, it is relevant to ask if the cis-isomer plays any role in dissociative adsorption of CH_3SSCH_3/Cu(111) because the probabilities of dissociation and isomerization of trans-CH_3SSCH_3/Cu(111) are comparable due to the similarity of the activation barrier of these two reactions. The role of the cis-isomer in this matter can be ruled out with our computational results which show the activation energy of the dissociation pathway of cis-CH_3SSCH_3/Cu(111) to be 0.11 eV. The effective total dissociation activation energy of the overall pathway comprising "trans-CH_3SSCH_3/Cu(111) via cis-CH_3SSCH_3/Cu(111) to $2CH_3S$/Cu(111)" is 0.34 eV, which is not insignificantly higher than 0.21 eV for direct dissociation of trans-CH_3SSCH_3/Cu(111) with no isomerization. In short, at low cryogenic temperature such as 5 K, CH_3SSCH_3/Cu(111) should show only top-site adsorption of trans-CH_3SSCH_3 with no isomerization and no dissociation, which coincides with known experimental results. At a moderate temperature such as room temperature, while the relative population of cis-CH_3SSCH_3/Cu(111) derived from the energy differential between the trans- and cis-isomer should still be merely about 0.01%, the dissociation channel with an activation barrier of 0.21 eV is wide enough for the exothermic dissociation to proceed. It is interesting that dissociation products of CH_3S/Cu(111) were found with a threshold temperature of 150 K,[8,21] but the probability of dissociation at 150 K through an activation barrier of 0.21 eV is still extremely low. Plausibly, the observed dissociation was mediated by intrinsic defects, as surface reconstructions were also observed under similar adsorption condition.[21] In this work, we did explore by computation if adsorption of CH_3SSCH_3/Cu(111) can induce the formation of intrinsic defects; our preliminary results indicate that at least for the low coverage of 1/16 and 1/20 monolayer nondissociative adsorption of trans-CH_3SSCH_3/Cu(111) does not cause any defect formation. A thorough follow-up work in this context is underway.

3.3. Preliminary Discussion on the Effects of Adsorption Coverage. To make a preliminary probe of the effects of coverage, we compare our computation results for a coverage of 1/16 monolayer (with a 4 × 4 supercell) with those for 1/20 (with a 4 × 5 supercell). It turns out that for both trans- and cis-CH_3SSCH_3/Cu(111) the reduction in coverage merely changes the S−S distance by ∼0.1 Å, and the C−S−S−C dihedral angle by ∼0.3°, with no change in the S−Au distances. The energy difference between the cis- and trans-CH_3SSCH_3/Cu(111) is 0.23 eV at a coverage of 1/16, and this changes to 0.22 eV at a coverage of 1/20.

Additionally, the MEP for the isomerization from trans-CH_3SSCH_3 to cis-CH_3SSCH_3 on Cu(111) is very similar to that at coverage of 1/16, the barrier being about 0.22 eV, which is smaller than that at coverage of 1/16 by 0.01 eV. Moreover, we further checked the effect of coverage on the dissociation reaction. As shown in Figure 6a, the MEP at coverage of 1/20 is almost the same as the one at coverage of 1/16 shown in Figure 5a. The transition state shown in Figure 6b is similar to that shown in Figure 5c. And the barrier is about 0.22 eV, which is larger than the barrier at coverage 1/16 by 0.01 eV. Our calculations show that at low coverage region both the

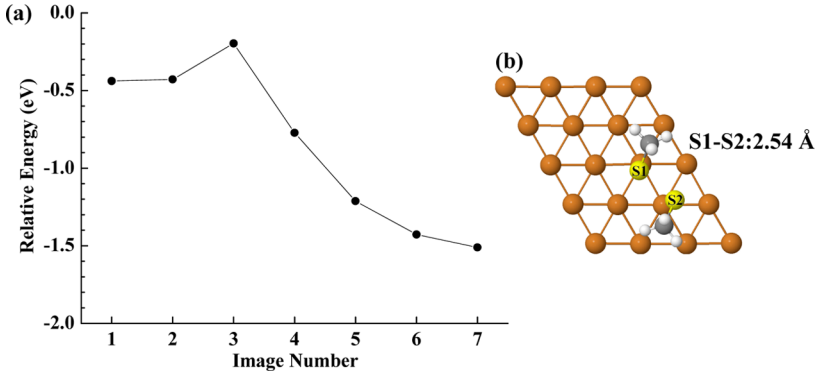

Figure 6. (a) Minimum energy path for the dissociation of the trans-CH_3SSCH_3 molecule on Cu(111) at coverage of 1/20. (b) Top view of the transition state.

dx.doi.org/10.1021/jp311481d | J. Phys. Chem. C 2013, 117, 6587−6593

geometry and energy of the nondissociative adsorption of CH_3SSCH_3 as well as the relevant reactions change little.

4. CONCLUSIONS

By performing a comprehensive search of all possible adsorption configurations, we clarify the nature of nondissociative adsorption of CH_3SSCH_3 on Cu(111), particularly the articulation of the relatively stable adsorption configurations of trans-CH_3SSCH_3 relative to its cis-counterpart. The most stable adsorption configuration of trans-CH_3SSCH_3 has the S atoms locating on two adjacent top sites of Cu(111), with the S−S bond aligning along the Cu−Cu bond. The adsorption energy is 0.42 eV. The rotational motion of methyl group of the adsorbed CH_3SSCH_3 transforms the trans-conformer to its cis-isomer, but this process is endothermic by 0.23 eV. Our calculated electronic structure further illustrates the formation of chemical bonds and the chemisorption nature of trans-CH_3SSCH_3/Cu(111). Moreover, our simulated STM images for the adsorption of trans-CH_3SSCH_3 match well with the experimental observation, which supports the validity of the adsorption model derived from our calculations.

In addition, this work also clarifies the detailed transition mechanisms from nondissociative adsorption of CH_3SSCH_3 to the dissociative adsorption of CH_3S. Along the minimum energy paths, the S−S bond of CH_3SSCH_3 dissociates and the two CH_3S units move away from each other along the S−S bond axis, and the directions of the S−C bonds are kept in reference to those in CH_3SSCH_3 prior to its dissociation. The activation barrier to dissociate the adsorbed trans-CH_3SSCH_3 is 0.21 eV, and the dissociation reaction is exothermic by 1.1 eV. These results explain that at a low coverage and cryogenic temperature CH_3SSCH_3/Cu(111) will stably assume the top-site nondissociative adsorption configuration in the trans-conformation. At moderate temperature such as room temperature, the activation energy of 0.21 eV is no longer high enough to block the dissociation of CH_3SSCH_3 and the formation of adsorbed CH_3S can proceed.

AUTHOR INFORMATION

Corresponding Author

*E-mail: xlfan@nwpu.edu.cn (X.-L.F.); leolau@csrc.ac.cn (W.-M.L.).

Notes

The authors declare no competing financial interest.

ACKNOWLEDGMENTS

This work was funded by the National Natural Science Foundation of China (NSFC) (20903075, 21273172) for Xiao-Li Fan. This work was also supported by the 111 Project (B08040) and 973 Project (2011CB922200) in China. The authors also acknowledge the generous support from the Beijing Computational Science Research Center, the Chengdu Green Energy and Green Manufacturing Technology R&D Center, the Institute of Chemical Materials, the Chengdu Development Center for Science and Technology, and the China Academy of Engineering Physics.

REFERENCES

(1) Love, J. C.; Estroff, L. A.; Kriebel, J. K.; Nuzzo, R. G.; Whitesides, G. M. *Chem. Rev.* **2005**, *105*, 1103−1169.
(2) Schreiber, F. *Prog. Surf. Sci.* **2000**, *65*, 151−256.
(3) Schwartz, D. K. *Annu. Rev. Phys. Chem.* **2001**, *52*, 107−137.
(4) Vericat, C.; Vela, M. E.; Salvarezza, R. C. *Phys. Chem. Chem. Phys.* **2005**, *7*, 3258−3268.
(5) Hasan, M.; Bethell, D.; Brust, M. *J. Am. Chem. Soc.* **2002**, *124*, 1132−1133.
(6) Zhou, J. G.; Hagelberg, F. *Phys. Rev. Lett.* **2006**, *97*, 045504−045507.
(7) Nenchev, G.; Diaconescu, B.; Hagelberg, F.; Pohl, K. *Phys. Rev. B* **2009**, *80*, 081401−081404.
(8) Bao, S.; McConille, C. F.; Woodruff, D. P. *Surf. Sci.* **1987**, *187*, 133−143.
(9) Porter, M. D.; Bright, T . B.; Allara, D. L.; Chidsey, C. E. D. *J. Am. Chem. Soc.* **1987**, *109*, 3559−3568.
(10) Ohara, M.; Kim, Y.; Kawai, M. *Langmuir* **2005**, *21*, 4779−4781.
(11) Maksymovych, P.; Yates, J. T. *J. Am. Chem. Soc.* **2006**, *128*, 10642−10643.
(12) Maksymovych, P.; Sorescu, D. C.; Yates, J. T. *Phys. Rev. Lett.* **2006**, *97*, 146103−146106.
(13) Rzeznicka, I. I.; Lee, J. S.; Maksymovych, P.; Yates, J. T. *J. Phys. Chem. B* **2005**, *109*, 15992−15996.
(14) Maksymovych, P.; Sorescu, D. C.; Dougherty, D.; Yates, J. T. *J. Phys. Chem. B* **2005**, *109*, 22463−22468.
(15) Nenchev, G.; Diaconescu, B.; Hagelberg, F.; Pohl, K. *Phys. Rev. B* **2009**, *80*, 081401−081404.
(16) Cometto, F. P.; Parredes-Olivera, P.; Macagno, V. A.; Patrito, E. M. *J. Phys. Chem. B* **2005**, *109*, 21737−21748.
(17) Lustemberg, P. G.; Martiarena, M. L.; Martinez, A. E.; Busnego, H. F. *Langmuir* **2008**, *24*, 3274−3279.
(18) Tielens, F.; Santos, E. *J. Phys. Chem. C* **2010**, *114*, 9444−9452.
(19) Fan, X. L.; Chi, Q.; Liu, C.; Lau, W. M. *J. Phys. Chem. C* **2011**, *116*, 1002−1011.
(20) Vericat, C.; Vela, M. E.; Benitez, G.; Carro, P.; Salvarezza, R. C. *Chem. Soc. Rev* **2010**, *39*, 1805−1834.
(21) Driver, S. M.; Woodruff, D. P. *Surf. Sci.* **2000**, *457*, 11−23.
(22) Hayashi, H.; Morikawa, T.; Nozoye, H. *J. Chem. Phys.* **2001**, *114*, 7615−7621.
(23) Grönbeck, H.; Curioni, A.; Andreoni, W. *J. Am. Chem. Soc.* **2000**, *122*, 3839−3842.
(24) Wang, Y.; Hush, N. S.; Reimers, J. R. *J. Am. Chem. Soc.* **2007**, *129*, 14532−14533.
(25) Woodruff, D. P. *Phys. Chem. Chem. Phys.* **2008**, *10*, 7211−7221.
(26) Vocnyy, O.; Dubowski, J. J.; Yates, J. T.; Maksymovych, P. *J. Am. Chem. Soc.* **2009**, *131*, 12989−12993.
(27) Maksymovych, P.; Vocnyy, O.; Dougherty, D. B.; Sorescu, D. C.; Yates, J. T. *Prog. Surf. Sci.* **2010**, *85*, 206−240.
(28) Ferral, A.; Patrito, E. M.; Parredes-Olivera, P. *J. Phys. Chem. B* **2006**, *110*, 17050−17060.
(29) Tielens, F.; Costa, D.; Humblot, V.; Pradier, C. M. *J. Phys. Chem. C* **2008**, *112*, 182−190.
(30) Tielens, F.; Humblot, V.; Pradier, C. M.; Calatayud, M.; IIIas, F. *Langmuir* **2009**, *25*, 9980−9985.
(31) Luque, N. B.; Santos, E.; Andres, J.; Tielens, F. *Langmuir* **2011**, *27*, 14514−14521.
(32) Fan, X. L.; Zhang, C.; Liu, Y.; Lau, W. M. *J. Phys. Chem. C* **2012**, *116*, 19909−19917.
(33) Paterson, S.; Allision, W.; Hedgeland, H.; Ellis, J.; Jardine, A. P. *Phys. Rev. Lett.* **2011**, *106*, 256101−256104.
(34) Kresse, G.; Furthmüller, J. *Phys. Rev. B* **1996**, *54*, 11169−11186.
(35) Kresse, G.; Furthmüller, J. *Comput. Mater. Sci.* **1996**, *6*, 15−50.
(36) Kresse, G.; Hafner, J. *Phys. Rev. B* **1993**, *47*, 558−561.
(37) Kresse, G.; Hafner, J. *Phys. Rev. B* **1994**, *49*, 14251−14269.
(38) Hohenberg, P.; Kohn, W. *Phys. Rev. B* **1964**, *136*, B864−B871.
(39) Kohn, W.; Sham, L. J. *Phys. Rev.* **1965**, *140*, A1133−A1138.
(40) Kresse, G.; Joubert, D. *Phys. Rev. B* **1999**, *59*, 1758−1775.
(41) Blochl, P. E. *Phys. Rev. B* **1994**, *50*, 17953−17979.
(42) Perdew, J. P. In *Electronic Structure of Solids '91*; Ziesche, P., Eschrig, H., Eds.; Academie-Verlag: Berlin, 1991; p 11.
(43) Tersoff, J.; Hamann, D. R. *Phys. Rev. B* **1985**, *31*, 805−813.
(44) Jónsson, H. *Annu. Rev. Phys. Chem.* **2000**, *51*, 623−653.

(45) Henkelman, G.; Uberuaga, B. P.; Jonsson, H. *J. Chem. Phys.* **2000**, *113*, 9901−9904.
(46) *American Institute of Physics Handbook*; McGraw-Hill: New York, 1979.
(47) Jiao, D.; Barfield, M.; Combariza, J. E.; Hruby, V. J. *J. Am. Chem. Soc.* **1992**, *114*, 3639−3643.
(48) Sutter, D.; Dreizler, H.; Rudolph, H. D. *Z. Naturforsch.* **1965**, *20a*, 1676−1681.
(49) Beagley, B.; McAloon, K. T. *Trans. Faraday Soc.* **1971**, *67*, 3216−3222.
(50) Fan, X. L.; Zhang, Y. F.; Lau, W. M.; Liu, Z. F. *Phys. Rev. Lett.* **2005**, *94*, 016101−016104.